Estuaries and Coasts
DOI 10.1007/s12237-012-9526-7

Submarine Groundwater Discharge-Derived Nutrient Loads to San Francisco Bay: Implications to Future Ecosystem Changes

Kimberly A. Null · Natasha T. Dimova · Karen L. Knee · Bradley K. Esser · Peter W. Swarzenski · Michael J. Singleton · Mark Stacey · Adina Paytan

Received: 11 December 2011 / Revised: 10 May 2012 / Accepted: 30 May 2012

Abstract Submarine groundwater discharge (SGD) was quantified at select sites in San Francisco Bay (SFB) from radium (^{223}Ra and ^{224}Ra) and radon (^{222}Rn) activities measured in groundwater and surface water using simple mass balance box models. Based on these models, discharge rates in South and Central Bays were 0.3–7.4 m^3 day^{-1} m^{-1}. Although SGD fluxes at the two regions (Central and South Bays) of SFB were of the same order of magnitude, the dissolved inorganic nitrogen (DIN) species associated with SGD were different. In the South Bay, ammonium (NH_4^+) concentrations in groundwater were three-fold higher than in open bay waters, and NH_4^+ was the primary DIN form discharged by SGD. At the Central Bay site, the primary DIN form in groundwater and associated discharge was nitrate (NO_3^-). The stable isotope signatures ($\delta^{15}N_{NO3}$ and $\delta^{18}O_{NO3}$) of NO_3^- in the South Bay groundwater and surface waters were both consistent with NO_3^- derived from NH_4^+ that was isotopically enriched in ^{15}N by NH_4^+ volatilization. Based on the calculated SGD fluxes and groundwater nutrient concentrations, nutrient fluxes associated with SGD can account for up to 16 % of DIN and 22 % of DIP in South and Central Bays. The form of DIN contributed to surface waters from SGD may impact the ratio of NO_3^- to NH_4^+ available to phytoplankton with implications to bay productivity, phytoplankton species distribution, and nutrient uptake rates. This assessment of nutrient delivery via groundwater discharge in SFB may provide vital information for future bay ecological wellbeing and sensitivity to future environmental stressors.

Keywords Submarine groundwater discharge · Radium · Radon · Estuaries · Nutrient loading · San Francisco Bay

K. A. Null (✉) · N. T. Dimova (✉) · A. Paytan
Institute of Marine Sciences, University of California Santa Cruz, Santa Cruz, CA, USA
e-mail: kimberly.null@gmail.com
e-mail: natodi@gmail.com

N. T. Dimova
Department of Geological Sciences, University of Alabama, Tuscaloosa, AL, USA

K. L. Knee
Smithsonian Environmental Research Center, Edgewater, MD, USA

B. K. Esser · M. J. Singleton
Lawrence Livermore National Laboratory, Livermore, CA, USA

P. W. Swarzenski
US Geological Survey, Pacific Coastal and Marine Science Center, Santa Cruz, CA, USA

M. Stacey
Department of Civil and Environmental Engineering, University of California Berkeley, Berkeley, CA, USA

Introduction

Submarine groundwater discharge (SGD) transports nutrients and other chemical constituents to receiving waters in many different coastal environments (e.g., Corbett et al. 1999; Slomp and Van Cappellen 2004; Paytan et al. 2006; de Sieyes et al. 2008; Knee et al. 2010). In some locations, nutrient loading from SGD is greater than that from rivers and surface runoff (Valiela et al. 1992; Corbett et al. 1999; Garrison et al. 2003; Hwang et al. 2005; Swarzenski et al. 2007; Knee et al. 2008). SGD flux and chemical

Published online: 28 June 2012

composition are spatially and temporally variable, and therefore, the impacts of SGD on water quality and ecology are site-specific (Taniguchi et al. 2002; Moore 2010). With increased coastal eutrophication worldwide due to densely populated coastlines and increasing demand on coastal resources (Paerl 2009), it is critical to assess SGD fluxes and evaluate their impact on coastal systems.

SGD to the coastal ocean includes both terrestrially derived freshwater and recirculated seawater from tidal and wave pumping, density differences, and bioirrigation (Burnett et al. 2003; Michael et al. 2005; Taniguchi et al. 2006). At many sites worldwide, particularly in arid or semi-arid locations where freshwater recharge is limited or groundwater is overdrawn, recirculated seawater may account for a significant component of SGD (Burnett et al. 2003; Shellenbarger et al. 2006; Taniguchi et al. 2006, 2007; Swarzenski and Izbicki 2009). Although the volume contribution of SGD to coastal and estuarine systems is typically much smaller than that of surface runoff (rivers, streams, etc.), the nutrient loading via SGD can be greater because groundwater is often enriched in nutrients and other materials relative to surface water (Null et al. 2011). Therefore, SGD can account for a large fraction of nutrient loading to a coastal system even when its contribution to the water budget is significantly lower (e.g., Valiela et al. 1990; Slomp and Van Cappellen 2004; Shellenbarger et al. 2006; Swarzenski et al. 2007; Knee et al. 2008; Breier et al. 2009).

Naturally occurring radium (Ra) and radon (Rn) isotopes are recognized as valuable geochemical tracers of SGD in estuaries and coastal environments because they are considerably elevated in groundwater compared to surface water (Moore 1996, 2010; Burnett and Dulaiova 2003; Charette et al. 2001; Swarzenski et al. 2007). ^{222}Rn activities can be related to total groundwater discharge (Burnett and Dulaiova 2003; Burnett et al. 2006), and radium isotopes, specifically ^{223}Ra and ^{224}Ra, are ideal tracers of brackish groundwater input and can be used to estimate water mass ages on the continental shelf (Moore 1999, 2000; Charette et al. 2001; Krest and Harvey 2003; Burnett et al. 2006; Moore and de Oliveira 2008; Moore 2010).

Previous work in San Francisco Bay (SFB) has modeled Rn benthic exchange from sediments to the overlying water column with focus on molecular diffusion and bioirrigation (Hammond and Fuller 1979; Hartman and Hammond 1984; Hammond et al. 1985). Based on Rn porewater profiles, the studies demonstrate that advective processes (i.e., irrigation) must occur in addition to molecular diffusion. Porewater is exchanged to depths of >40 cm in the sediments at some locations in SFB with advective flux estimated to account for 60 % of benthic exchange when considering bioirrigation compared to diffusional fluxes (Hammond et al. 1985). These studies indicate that SGD, mostly as recirculated seawater discharged through bioirrigation of sediments in SFB, is prevalent; however, other processes that may contribute to SGD and associated nutrient fluxes such as tidal pumping, wave action, salt dispersion, and seasonal oscillations were not accounted for and could be important (Michael et al. 2005).

We examined SGD and the associated nutrient fluxes in South and Central San Francisco Bay, California, using the activities of two radium isotopes (^{223}Ra and ^{224}Ra) and the temporal and spatial distribution of radon (^{222}Rn) activity. For the purpose of this study, SGD is defined as the total SGD flux regardless of the forcing mechanisms such as bioirrigation, diffusion, or other physical forces impacting seawater recirculation (i.e., tidal pumping, hydraulic head, wave action) as well as any meteoric fresh groundwater discharge. Fluxes of groundwater were evaluated using Ra and Rn activities and a simple box model that constrained all input and removal functions for these radionuclides in a coastal water column. SGD-derived nutrient fluxes were compared to other nutrient sources to determine the relative nutrient contribution from SGD and their role in future ecosystem changes.

Study Sites

The SFB and Delta estuarine system is the largest estuary on the Pacific coast of the USA and is one of the most impacted systems due to anthropogenic activities (Nichols et al. 1986; Kennish 2001). The heavily populated SFB area (approximately seven million people) puts stress on aquatic ecosystems with groundwater withdrawal, agriculture activities, and wastewater discharge. Ninety percent of freshwater input to SFB flows from the Sacramento–San Joaquin River Delta with the remaining 10 % of freshwater from seasonal local streams, sewage input, and unquantified groundwater discharge (Porterfield et al. 1961; Conomos et al. 1985). South and Central Bays are both influenced by Delta flows, but the effects are lagged and dramatically reduced in South Bay compared to Central Bay (Conomos et al. 1985).

The SFB ecosystem is undergoing changes (increased chlorophyll concentrations, larger algal blooms, new seasonal blooms, and grazing intensity) (Cloern et al. 2007), and few studies regarding the role of SGD in SFB water quality and ecosystem health have been conducted, particularly with respect to the understanding of the SGD relationship to these changes. Previous studies focused on the impact of bioirrigation on SFB water quality (Hammond et al. 1985), but many of the studies have been conducted prior to the more recent documented changes in the bay ecosystem. The current understanding of productivity in the bay is that phytoplankton blooms are limited by light caused by high turbidity in bay waters and increased grazing by introduced bivalves (Alpine and Cloern 1992; Cloern et al.

2007). Phytoplankton biomass increased in SFB after 1999 due to a decline in bivalve populations from a climatically driven increase in bivalve predator populations (Cloern et al. 2007). This increase in phytoplankton biomass demonstrates that SFB is not immune to nutrient pollution and changes in bay conditions can inherently increase the use of the current large stock of nutrients in bay waters. Other changes such as water clarity can also influence conditions in SFB, and thus, its ecosystem may change as a result of sudden decrease in suspended-sediment concentration (Schoellhamer 2011). An increase in water clarity could eventually transition the SFB to a nutrient-limited system that will increase ecosystem sensitivity to nutrient inputs and nutrient stoichiometry, both of which may be significantly influenced by SGD. Despite decades of water quality and ecosystem monitoring work in SFB (Baylosis et al. 1997; Cloern et al. 2000), few estimates (Hammond et al. 1985; Spinelli et al. 2002) and no direct measurements of the contribution of total SGD (i.e., including recirculated seawater, tidal pumping, and wave action) to the system exist. Such estimates are especially important in view of the current and predicted changes in sea level, rainfall, and demand on freshwater sources in the bay (Knowles and Cayan 2002).

Work reported here took place at three sites in South and Central SFB representing different coastal settings common to the entire SFB region (Fig. 1). Two sites, Marine Science Institute (MSI) and Palo Alto Baylands State Park (PA), were located in South SFB (referred to as South Bay hereafter), and the other site, Angel Island (AI), was located in Central SFB (Central Bay). The hydrogeology of the study sites (described below), in terms of the surrounding topographic relief, sediment characteristics, and coastal morphology, represents vast areas throughout the South and Central Bays.

South Bay is a shallow embayment that has a maximum depth of ~10 m in the channel and average depth of ~4.5 m (http://sfbay.wr.usgs.gov). South Bay receives very little freshwater from tributaries and has a water residence time of several months during summer and approximately 30 days during winter (Walters et al. 1985). Circulation in South Bay is set by the interplay of tidal forcing modified by wind-forcing and intermittent density forcing due to freshwater from Central Bay, wastewater discharge, and small streams (Conomos et al. 1985). South Bay is also tremendously modified and impacted by dense population and infrastructure; for example, sewage discharge from wastewater treatment facilities is a major source of freshwater to South Bay (Conomos et al. 1985). The South Bay shoreline generally consists of fine-grained sediments and has a long coastal line that is dendritic and highly complex encompassing many sloughs and ponds. The seafloor in this part of the bay is composed mostly of silt and clay sediments

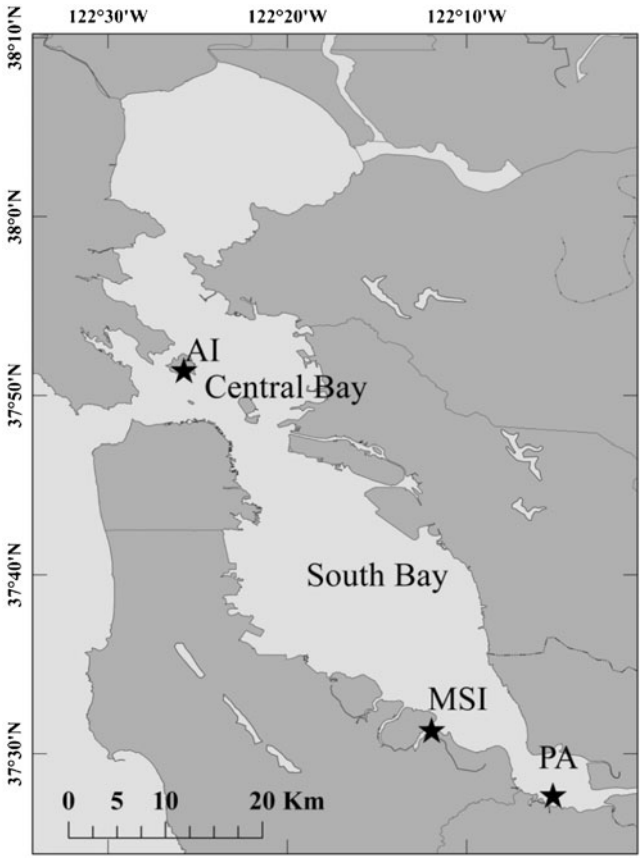

Fig. 1 Map of San Francisco Bay and three sampling locations (Marine Science Institute (*MSI*), Palo Alto Baylands (*PA*), and Angel Island (*AI*))

(Conomos and Peterson 1977; Chin et al. 2010). At PA, two different intertidal and nearshore (including part of the subtidal zone) settings were investigated, one in a slough environment (PA–SP) and one adjacent to open bay waters (PA–NC). Samples for the nearshore (water depth up to 1.5 m at high tide) were collected from the surface (upper 0.5 m) at each location. Samples were collected from the intertidal area during low tide from wells installed to intersect the water table (water pumped from the upper 30 cm of the water table depth). The water table depth was approximately the same depth at a site at any given sampling time but varied between sites and tidal stages. PA and MSI are located on the west side of the South Bay with flat topography (<1 % slope calculated from the difference in elevation from the water line to 5 km inland using a topography map) that includes salt marshes and sloughs, and both sites are characterized by a broad tidal zone with shallow gradients. The beaches sampled in the South Bay, in the slough and adjacent to open bay, encompassed less than 1 km in length of beach, but similar broad, shallow intertidal zones exist along majority of the perimeters of South Bay.

The Central Bay site (AI) is located on the west side of Angel Island and is characterized by considerable relief

(~4–10 % east Central Bay and 26 % gradient west Central Bay calculated from the difference in elevation from the water line to 5 km inland using a topography map). At AI, the intertidal and nearshore setting was investigated at a beach of approximately 1 km length located in a cove with a shallow gradient. The topographic relief of Central Bay creates substantial hydraulic head gradients from land to sea and a smaller area that is impacted by tidal inundation compared to South Bay. The average water depth in Central Bay is 13.4 m, which is deep compared to the rest of SFB (~6 m) (http//:sfbay.wr.usgs.gov). Water in Central Bay is primarily composed of coastal Pacific water, which is influenced to various degrees by Delta water contribution. Density gradient drives estuarine circulation, and water residence time is on the order of days during high river discharge periods and up to months during the dry season (Walters et al. 1985). The surrounding coastline is comprised of sandstone and shale along a narrow shoreline, and the Central Bay seafloor is comprised mostly of sand and silty sand (Conomos and Peterson 1977; Chin et al. 2010).

Methods

Surface water and groundwater samples were collected from each of our sampling sites (Fig. 1) on several field campaigns between March 2009 and May 2010. MSI was sampled in March and April 2009; PA was sampled in March 2009, October 2009, and May 2010; and AI was sampled in May 2010. The tides in SFB are semi-diurnal mixed, and samples were collected over varying tidal stages at each site. The tides in South Bay near MSI and PA averaged 2.2 m for high and 0.4 m for low tides during all sampling days. At AI, high tides and low tides were 1.5 and 0.3 m, respectively (NOAA tide predictions; http://tbone.biol.sc.edu/tide/worldmap.html).

At each location, surface water and groundwater samples were collected along shore-perpendicular transects. Each transect consisted of at least six discrete samples, three from temporary screened PVC wells installed at the beach face to the water table (up to 1.25 m depth to the groundwater sampled depending on the site) and three or more from surface water at increasing distance from shore up to 20 m offshore. The water table depth at the wells was approximately the same at a site but varied between sites. Water from within the sloughs, if present, was also collected. Surface water samples from the mid-channel of the Bay were collected from surface and bottom water via a boat using a submersible pump and were used to represent the offshore (Bay water) Ra end-member (see flux calculations in the following section). Samples were analyzed for a suite of parameters including ^{223}Ra, ^{224}Ra, ^{222}Rn, nutrients ($NO_3^-+NO_2^-$, NH_4^+, PO_4^{3-}, $Si(OH)_4$), and nitrate isotopic composition ($\delta^{15}N_{NO3}$ and $\delta^{18}O_{NO3}$). Water quality parameters (salinity, conductivity, temperature) were measured in the field using a handheld YSI 85 multi-probe previously calibrated in the laboratory. In addition, we performed continuous surveys of Rn, temperature, and salinity in the surface water along the coast of South Bay.

Radium Activity

Groundwater and surface water samples (40 and 100 L each sample, respectively) were collected using submersible pumps and passed through MnO_2-coated acrylic fiber at a flow rate <2 L min^{-1} to quantitatively scavenge the Ra isotopes (Moore 1976). ^{223}Ra and ^{224}Ra activities were measured using a delayed coincidence counter (RaDeCC) (Moore and Arnold 1996). The fibers were analyzed twice: immediately after collection and approximately 4 weeks after collection to assess ^{228}Th and correct for supported ^{224}Ra (Moore and Arnold 1996; Moore 2003). Standards were run on a monthly basis as part of the quality control protocol of the instrument. The analytical error of the calculated efficiencies of the RaDeCC systems is typically <10 %. The average error associated with the measurement of ^{224}Ra and ^{223}Ra activities for all samples is 10 and 26 %, respectively. Error in measured activities was calculated based on Garcia-Solsona et al. (2008).

Radon Activity

Rn activities were measured continuously for ~24 h (at least three tidal cycles) using a RAD7 radon-in-air monitor with RAD-AQUA accessory (Durridge, Inc) in one well and one surface water location at each site: at MSI in April 2009, at PA in October 2009, and at AI in May 2010. The samples were pumped from ~0.3 m below the water table at a rate <1 L min^{-1} for Rn analysis. Detailed information about this instrumentation can be found elsewhere (Burnett and Dulaiova 2003). In all cases, Rn data were recorded in 30-min intervals. Using this time interval, observed analytical errors were 10–15 %, depending on the measured activities in water. Analytical errors for groundwater samples were consistently below 10 % as the measured Rn activities in groundwater were much higher than in surface water. Conductivity, temperature, and depth loggers (Van Essen instruments®) were deployed at each location to monitor water level and salinity changes throughout the Rn data collection period. Surface water surveys of Rn were conducted from a boat following the coastline of South Bay during March 2009 to map surface water Rn distribution in South Bay (the sample locations for the Rn transect are those shown in Fig. 4).

Nutrient Concentration and Nitrate Isotope Ratios

Samples for nutrient concentrations ($NO_3^-+NO_2^-$, NH_4^+, PO_4^{3-}, $Si(HO)_4$) were filtered with 0.45 μm cartridge filters and collected in acid cleaned polyethylene

bottles. Samples were frozen until analysis. Analyses were done using a Lachat Quickchem 8000 Flow Injection Autoanalyzer at UCSC. Instrument error was <9 % for all nutrients based on duplicates analyzed every ten samples.

Samples for isotopic composition of nitrate ($\delta^{15}N_{NO3}$ and $\delta^{18}O_{NO3}$) were filtered (0.45 μm) in the field and kept frozen until analysis. Samples were analyzed following a version of the denitrifier method (Sigman et al. 2001; Singleton et al. 2005). Isotopic analysis was conducted at Lawrence Livermore National Laboratory on an IsoPrime continuous-flow mass spectrometer. Analytical precision for both $\delta^{15}N_{NO3}$ and $\delta^{18}O_{NO3}$ is 0.5 ‰. The denitrifier method provides the results of the combined NO_3^- and NO_2^- signatures and not solely NO_3^- (Wankel et al. 2006). However, NO_2^- in our samples contributes much less than 5 % of total oxidized nitrogen; thus, the impact of NO_2^- on the measured isotopic signatures is expected to be small and is ignored here. Nitrate and nitrite were measured together and will be reported as $NO_3^-+NO_2^-$ hereafter.

SGD Flux Calculations

The SGD fluxes (cubic meters per day per meter) were calculated based on the excess tracer (Ra and Rn) activities in the bay using established mass balance models (Moore 1996; Burnett and Dulaiova 2003). Two different scales for the mass balance model were used to estimate SGD in South and Central Bays: (1) a nearshore model: modeling the flux into a nearshore prism for each site (1 m along shore × 20 m offshore × 1.5 m maximum depth) and (2) a bay basin model: modeling the combined basins of the South and Central Bays using volume estimates from Smith and Hollibaugh (2006). The first calculation provides a flux estimate representative of a specific shoreline length to the nearshore environment. The distance of shore defining the near shore box was selected based on the distance where there was no measurable excess Ra compared to the offshore end-member (the middle of the bay). SGD flux calculations are sensitive to the selected size of the box; for example, if excess Ra is elevated to the same level at 30 m offshore, the calculated flux would be 45 % higher. If the discharge zone extends more than 20 m offshore, our calculations will constitute a conservative estimate particularly because about 80 % of the bay is classified as shallow shoals (Hammond et al. 1985). These nearshore fluxes were extrapolated to the entire bay basin (South or Central) assuming these sites are representative of similar settings along each bays' coastlines. The second calculation using the bay basin model integrates the combined flux over the basin scale (South and Central). For the mass balance mixing calculations, the end-members used were groundwater (using temporally integrated average values) and either open bay water (for the nearshore model) or coastal Pacific seawater (for the bay basin model). The following equation was used to determine the SGD fluxes based on excess Ra activity in the nearshore box (e.g., Moore 1996; Krest et al. 2000; Paytan et al. 2006):

$$D = \frac{(A_{\text{box}} - A_{\text{offshore}})V_{\text{box}}}{A_{\text{GW}}\tau} \quad (1)$$

Discharge (D) (cubic meters per day) per meter of shoreline is calculated from the excess activity (e.g., Ra activity above that of the offshore water) and therefore must be supplied from SGD; A_{box} is the average Ra activity in the box (disintegrations per minute per 100 L^{-1}); A_{offshore} is the offshore activity in the open bay or coastal Pacific waters for the nearshore box or bay basin calculations, respectively (disintegrations per minute per 100 L^{-1}); V_{box} is the volume of the model box. For the nearshore model, V_{box} is set at a 15 m^3 prism (1 m along shore × 20 m in the offshore direction × the average depth of 0.75 m; the maximum depth at 20 m is 1.5 m). For the bay basin model, V_{box} is set using volume estimates from Smith and Hollibaugh (2006). τ is the water residence time (days) and was estimated using two independent calculations (tidal prism replacement and apparent age of nearshore waters) to better constrain the value. The water residence time is estimated to be 1.03 day for the nearshore boxes based on 50 % of the volume of the box being exchanged with each tidal cycle, a value modeled from the fluxes of salinity and temperature (Hsu and Stacey 2011). We assume alongshore transport is negligible. Residence times for the bay basin model for South and Central Bays were based on estimates from Walters et al. (1985) and considering salinity data obtained during sampling were set at 60 days. We note, however, that this bay scale water balance residence time does not consider fluxes related to recirculated bay water and recirculated submarine groundwater in the subterranean estuary (Robinson et al. 2006). Excess activity in the box (disintegrations per minute) was divided by the measured Ra activity of the groundwater end-member (A_{GW} disintegrations per minute per cubic meter) and the respective residence time to obtain an estimate of groundwater discharge (cubic meters per day). It was assumed the system is in steady state and therefore the decay term was not included in Eq. 1. The total discharge to South and Central Bays was calculated by multiplying the discharge per meter of shoreline derived from the nearshore model by the length of the shoreline of each basin in addition to estimating it using the basin scale model. The diffusional flux is not considered

independently in this calculation; rather, our model represents the net overall SGD flux regardless of forcing mechanism (see "Discussion").

We estimated the apparent age of nearshore waters independently, based on the difference in $^{224}Ra/^{223}Ra$ activity ratio (AR) between surface and groundwater (Moore 2000). This method assumes that discharging groundwater has a constant and uniform AR, so that AR changes as a result of radioactive decay as follows:

$$t = \ln\left(\frac{AR_{surf}}{AR_{GW}}\right)\frac{1}{(\lambda_{224} - \lambda_{223})} \quad (2)$$

where t is the apparent age of waters (days), AR_{surf} is the average surface water AR, and AR_{GW} is the average activity ratio of groundwater for each site; λ_{224} is the ^{224}Ra decay rate (0.191 day^{-1}) and λ_{223} is the ^{223}Ra decay rate (0.0608 day^{-1}). This calculation yields a water age of 1.31 day for the nearshore coast of AI, similar to the residence time based on tidal prism replacement time (1.03 day). The average nearshore apparent age determined using AR changes in South Bay is 3.7 days at MSI and 1.8 day at PA, slightly longer than the tidal prism estimates (1.03 days). We report a flux range that encompasses the various residence time estimates. We recognize that the Ra-based calculations account only for brackish SGD because low Ra freshwater discharge is not included; accordingly, this calculation might underestimate total SGD if freshwater discharge is significant. In South Bay, we do not expect significant freshwater discharge based on the saline nature of the groundwater observed and no evidence of channelized freshwater flow.

The Rn-derived groundwater fluxes presented here were calculated using a single-box Rn non-steady-state mass-balance model (Burnett and Dulaiova 2003). In this model, we monitor changes in Rn inventories over time (~3 tidal cycles in 30 min increments) while accounting for losses (via gas evasion, mixing with offshore water, and radioactive decay) and inputs (through groundwater and production from dissolved ^{226}Ra in the water column). The calculated Rn fluxes are then converted to an SGD rate by dividing by the groundwater end-member Rn activity. This approach has proven to be robust and has been used successfully in different coastal environments. Since the Rn activity in nearshore groundwater oscillated with the tidal cycle, only average maximum values of the detected Rn activities over multiple tidal cycles (usually associated with lowest salinity values) were used as the groundwater end-member in the Rn model for assessing discharge rates. Using the maximum groundwater Rn activity is a conservative approach to calculate SGD resulting in lower fluxes than if the whole data set is used (Burnett and Dulaiova 2003).

Statistical Analyses

Variance in sample type (groundwater, nearshore, and offshore) and among sampling locations were analyzed using Kruskal–Wallis nonparametric one-way analysis of variance. Correlation between samples and tides were determined using simple linear regression. Statistical significance was determined using a 95 % confidence interval with the probability (p)<0.05. All statistical analyses were conducted using StatCrunch (Integrated Analytics, LLC).

Results

Ra and Rn Activities

Averages and ranges of ^{224}Ra, ^{223}Ra, and ^{222}Rn activities for groundwater and surface water at the different sites are presented in Table 1. Groundwater ^{224}Ra activities were found to be in the range of 18.5–422 dpm 100 L^{-1} and ^{223}Ra activities in the range of 0.5–58.6 dpm 100 L^{-1}. Groundwater ^{224}Ra, ^{223}Ra, and ^{222}Rn activities were significantly higher (approximately three-fold) compared to surface water at all sites (p<0.0001). Figure 2 shows the ^{224}Ra and ^{223}Ra activities in groundwater and with distance offshore for each of the sampling locations. The groundwater activities are averages of activity measured in samples from each well (GW1, GW2, GW3) over the tidal cycle (Fig. 2). We did not observe a significant decrease in ^{224}Ra or ^{223}Ra activities with distance from shore between the waterline and 20 m (the seaward extent of our small nearshore box), suggesting the nearshore zone was well mixed on time scales representative by the Ra decay constants. The activities in nearshore bay waters (<20 m) were significantly higher (approximately two-fold) relative to open bay waters in South Bay (p<0.0001 for MSI and p=0.0003 for PA) (Table 1; Fig. 2). There was not a significant difference between nearshore and offshore activities at AI (p>0.05). Higher Ra activities in groundwater compared to surface water are typical to most coastal sites with brackish SGD (Moore 1999). The SGD flux was calculated based on averaged Ra activities for each sample type over all tidal stages because Ra activities did not correlate significantly with tidal stage (p>0.05).

$^{224}Ra/^{223}Ra$ AR in groundwater were similar (within analytical error) for all samples at the three study sites, indicating sources with similar AR contributing Ra to surface waters (Fig. 3). The ARs for samples within the small nearshore zones were significantly lower than that of groundwater (p<0.05 for MSI and PA) (Table 2). The AR for the open bay water was also significantly lower than that of the groundwater (p<0.0001 for MSI and PA; p<0.05 for

Table 1 ^{224}Ra, ^{223}Ra, and ^{222}Rn activity ranges and mean activity at each sampling location

Site		^{224}Ra (dpm 100 L^{-1})	^{223}Ra (dpm 100 L^{-1})	^{222}Rn (dpm L^{-1})
MSI	Groundwater	23.4–185 (63.3±39.3) n=17	0.7–15.6 (5.6±4.2) n=17	3.5–77.5 (28.6±22.4)
	Surface	14.5–27.2 (21.4±3.8) n=15	1.4–3.7 (2.7±0.8) n=15	2.6–7.4 (5.6±1.1)
PA (SP)	Groundwater	43.0–422 (170±142) n=10	1.3–32.6 (15.6±10.6) n=10	NA
	Surface	19.9–41.7 (34.3±8.0) n=6	2.5–4.6 (3.6±0.9) n=6	NA
PA (NC)	Groundwater	18.6–228 (128±86.2) n=5	0.5–18.1 (9.1±7.4) n=5	3.9–21.7 (9.7±4.4)
	Surface	17.3–53.8 (27.6±13.1) n=7	1.3–2.9 (2.1±0.7) n=7	3.8–10.2 (7.0±4.5)
PA (average)	Groundwater	51.9–228 (144±77.3) n=15	8.5–58.6 (22.2±20.8) n=15	NA
	Surface	17.3–110 (44.2±27.0) n=13	0.5–12.7 (4.0±2.9) n=13	NA
AI	Groundwater	18.5–92.2 (60.9±21.5) n=17	1.2–8.0 (4.7±1.8) n=17	0.7–29.0 (96.8±78.8)
	Surface	11.1–29.3 (15.4±4.9) n=29	1.0–2.1 (1.4±0.3) n=29	0.9–2.5 (1.6±0.3)
South Bay	Surface	6.8–13.2 (9.5±2.2) n=13	0.5–1.5 (1.2±0.3) n=13	
Central Bay	Surface	10.2–15.1 (12.5±1.5) n=11	0.7–1.6 (1.2±0.3) n=11	

PA includes two sampling sites (SP and NC) and the combined ranges and mean are also given as PA (average). South and Central Bay values represent the offshore surface water activities for each bay. Parentheses are means and ±1σ. Note ^{224}Ra and ^{223}Ra is in disintegrations per minute per 100 L^{-1} and ^{222}Rn in disintegrations per minute per liter

MSI Marine Science Institute, *PA* Palo Alto Baylands, *AI* Angel Island

AI), consistent with the longer residence time and the faster decay of ^{224}Ra relative to ^{223}Ra. There was no significant difference between the AR of the nearshore waters and open bay waters at AI (p>0.05). The lack of a significant difference between nearshore and offshore waters in AI is likely because we were not able to obtain samples greater than 500 m from the shoreline (due to boat limitations) or because of rapid mixing between the offshore and nearshore on time scales shorter than those captured by AR changes at this site.

The spatial distribution of ^{222}Rn in South Bay reveals the following general patterns: (1) Rn activities are generally low in open waters of SFB, (2) higher Rn activities were observed in some nearshore environments (Table 1), and (3) Rn was consistently the lowest in the very shallow southernmost stretch of South Bay (Fig. 4). Time-series trends of Rn in groundwater varied with the tide in all sampling sites and showed distinct inverse relation with tide, i.e., higher radon was observed during low tide compared to high tide (Fig. 5a). Similar trends, although dampened by mixing with offshore low radon concentration waters, were observed in surface waters at the nearshore sites indicative of tidal influence on Rn flux to surface water (Fig. 5b). These values are used to calculate the SGD flux over tidal cycles (Fig. 5c) in centimeters per day and described in the next section.

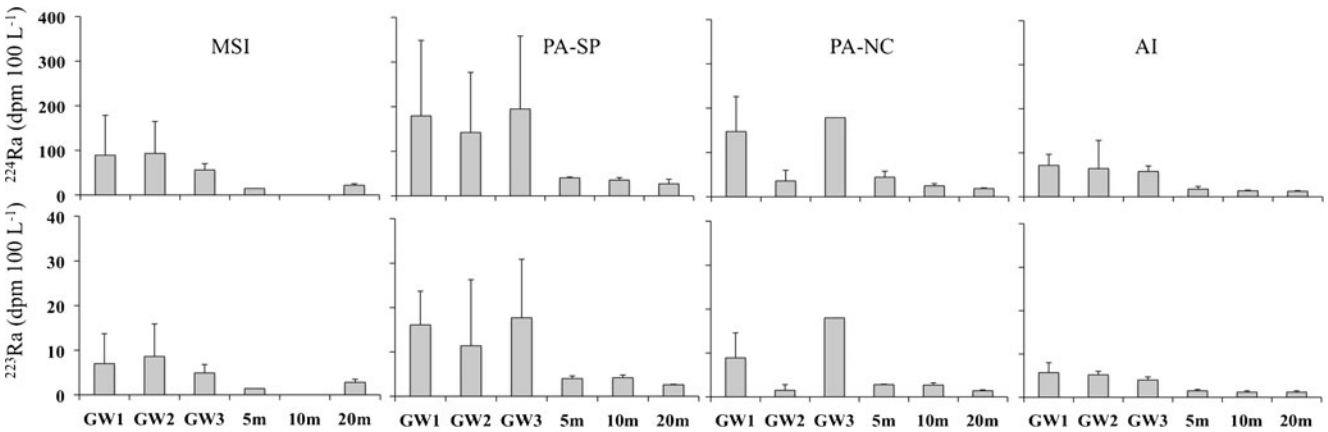

Fig. 2 **a** ^{224}Ra and **b** ^{223}Ra activities with distance from shore at the three sampling sites. Groundwater samples (*GW*) are from wells or pits in a transect to shoreline; distance varies between sites. The distance from shore for surface water samples (5, 10, and 20 m) are approximate. *Error bars* represent 1σ. *Error bars* are not shown for sample sets of n≤2

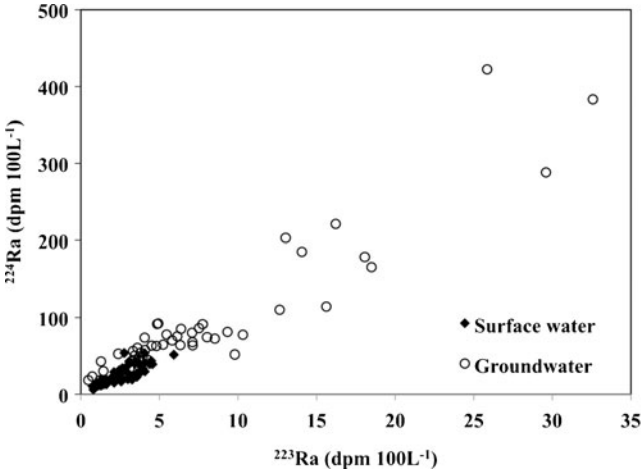

Fig. 3 ^{224}Ra versus ^{223}Ra activities in groundwater (n=42) and surface water (n=119) samples at all sampling locations

SGD Flux Estimates

The SGD fluxes at the different sites calculated from excess Ra activities and the nearshore box model are represented in Fig. 6. The SGD flux was calculated based on averaged Ra activities for each sample type (groundwater, coastal, and offshore) over all tidal stages because radium activities did not correlate significantly with tidal stage (p>0.05). The SGD fluxes per meter of shoreline calculated based on ^{224}Ra activities at the different South Bay sites were between 0.3 and 7.4 m^3 day^{-1} m^{-1} (mean 1.7 m^3 day^{-1} m^{-1}) and 0.7–6.0 m^3 day^{-1} m^{-1} (mean 1.6 m^3 day^{-1} m^{-1}) at MSI and PA (including both PA-SP and PA-NC), respectively (Fig. 6a). The range of SGD flux based on ^{224}Ra activities at AI in the Central Bay was 0.7–4.2 m^3 day^{-1} m^{-1} with a mean of 1.2 m^3 day^{-1} m^{-1} (Fig. 6a). The ranges represent the SGD flux calculated using the highest and lowest groundwater end-member activity and include SGD calculated independently using the two different residence time estimates. The means of SGD fluxes are calculated using the average groundwater Ra activities at each site. SGD fluxes calculated using ^{223}Ra produced similar mean fluxes: 2.5, 1.2, and 0.8 m^3 day^{-1} m^{-1} at MSI, PA, and AI respectively; the errors associated with the calculations based on ^{223}Ra are larger than those determined using ^{224}Ra (Fig. 6b).

The Rn activities of groundwater and surface water, corresponding tidal cycle, and calculated advection rates in centimeters per day are represented in Fig. 5. The SGD rates in centimeters per day calculated via the Rn model were converted to cubic meters per day per meter based on the same area of discharge used for the Ra model at each site and are: MSI up to 30 m^3 day^{-1} m^{-1} (with a groundwater end-member of 60 dpm L^{-1}); PA up to 2 m^3 day^{-1} m^{-1} (using 81.3 dpm L^{-1} for the groundwater end-member) and up to 210 m^3 day^{-1} m^{-1} (using 9.73 dpm L^{-1}); AI SGD flux was up to 6 m^3 day^{-1} m^{-1} (using an end-member of 300 dpm L^{-1}). Figure 5 shows the variation in Rn activities with the tidal cycles at AI, which are used to calculate the advection rate. The model showed similar impact of tidal fluctuations with peak Rn activities occurring near periods of low tide at the PA sites as well (data not shown). MSI had anonymously high Rn activities, and the water level record did not demonstrate the complete tidal variability.

Table 2 Activity ratios of ^{224}Ra and ^{223}Ra means and ±1σ for groundwater and nearshore surface water at each site and open bay water

Site		n	AR
MSI	Groundwater	17	12.9±5.4
	Surface	15	8.3±1.8
PA-SP	Groundwater	10	12.3±8.0
	Surface	6	9.7±2.0
PA-NC	Groundwater	5	21.1±11.0
	Surface	7	16.2±3.4
AI	Groundwater	17	13.3±2.6
	Surface	29	11.0±2.0
Bay	Surface	13	8.5±2.3

Nutrient Concentrations

Dissolved inorganic nitrogen (DIN including NH_4^+ and NO_3^-+NO_2^-) concentrations as well as PO_4^{3-} and $Si(OH)_4$ in SFB were considerably higher in groundwater compared to surface water (Table 3). Nutrient concentrations in both groundwater and surface water tended to be higher in the South Bay sites than at AI (Table 3), possibly due to the higher level of anthropogenic impact, larger volume of sewage discharge, and longer water residence time in the South Bay. We found that ^{224}Ra activity was positively correlated to NO_3^-+NO_2^-, NH_4^+, PO_4^{3-}, and $Si(OH)_4$ concentrations in groundwater and nearshore waters (<20 m). Specifically, ^{224}Ra activity in groundwater and nearshore water in South Bay was positively correlated to NO_3^-+NO_2^-, NH_4^+, and $Si(OH)_4$ but not PO_4^{3-} (p=0.02, p<0.0001, p=0.001, p>0.05, respectively). In Central Bay, all nutrients were significantly correlated to ^{224}Ra except NH_4^+ (p>0.05), probably due to the higher concentrations of NH_4^+ in surface waters at this site. The difference in correlation of ^{224}Ra and PO_4^{3-} between South and Central Bays may reflect the difference in redox conditions in the sediment.

The dual isotopic signature of NO_3^-+NO_2^- ($\delta^{15}N_{NO3}$ and $\delta^{18}O_{NO3}$) in groundwater and surface water at each site are plotted in Fig. 7. There was no significant difference in isotopic signature between groundwater and surface waters at any of the sites (Fig. 7). Our NO_3^-+NO_2^- isotopic values, $\delta^{15}N_{NO3}$ range of +3 to +14 ‰ and $\delta^{18}O_{NO3}$ range of −4 to +19 ‰, are similar to those reported by Wankel et al. (2006) for the entire bay ($\delta^{15}N_{NO3}$ range of +6.5 to +13.9 ‰ and

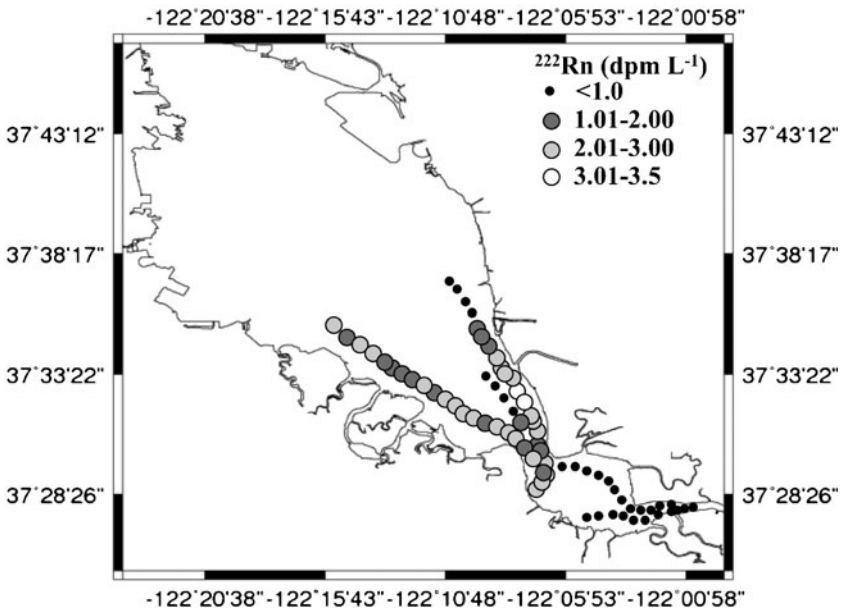

Fig. 4 Distribution of ^{222}Rn activities in surface water in South Bay during March 2009

$\delta^{18}O_{NO3}$ range of −5.0 to +11.6 ‰). However, the $\delta^{15}N_{NO3}$ and $\delta^{18}O_{NO3}$ values were significantly different between South Bay (MSI and PA) and Central Bay (AI) ($\delta^{15}N_{NO3}$ p=<0.001, $\delta^{18}O_{NO3}$ p=.005) (Fig. 7).

Discussion

Higher Ra activities in groundwater compared to surface water are typical to most coastal sites with brackish SGD (Moore 1999) and were found in all sites in this study conducted in SFB. Elevated Rn concentrations were also found in groundwater compared to surface water at our SFB sites, and therefore, we found Ra and Rn to be valuable tracers of SGD in SFB. These tracers along with the nutrient characteristics of groundwater at the different sites provide valuable insight to biogeochemical processes in the subterranean estuary which may have implications to SFB water quality and ecosystem structure as discussed in the sections below.

SGD Derived from the Nearshore Model

Both Ra and Rn models were used to derive two independent estimates of SGD flux of the nearshore intertidal sites. The Ra model produced SGD fluxes on the order of 1.7, 1.6, and 1.2 $m^3\ day^{-1}\ m^{-1}$, whereas the Rn model produced fluxes on the order of 30, 2, and 6 $m^3\ day^{-1}\ m^{-1}$ for MSI, PA, and AI, respectively. While using Ra as a SGD tracer yields information on the saline component of SGD, the Rn-derived SGD rates are representative of the total SGD (i.e., both fresh and recirculated water). At MSI, the SGD calculated using the Rn model produced an order of magnitude higher SGD flux than the Ra model; however, the Rn measurements at this site may have been compromised by local conditions during sampling resulting in higher than expected calculated fluxes. Specifically, it is likely that strong winds (up to 40 kph) during the October sampling diminished the effectiveness of Rn as a reliable SGD tracer at this site. At PA mean SGD flux calculated using Rn was within the same range as the SGD flux calculated using Ra, as expected with little freshwater contribution. The Rn-derived SGD values in South Bay are consistent with minimal freshwater discharge and illustrate the importance of recirculated seawater in this environment. At AI, the SGD flux based on Rn was higher compared to the SGD flux based on Ra, suggesting some contribution of freshwater inputs at this site (indeed fresher groundwater was encountered).

Conditions such as topographic relief can play an important role in SGD, seawater infiltration, subsurface flow, and the overall impact on transport mechanisms (Nakada et al. 2011). Saltwater infiltration can be intensified at the beach face of a low-relief estuary, but infiltration has been shown to be even stronger at tidal flat settings (Mao et al. 2006). Also, at tidal flat locations, there is evidence that a freshwater lens may not discharge offshore of the tidal flat like at a sloping beach face because of seawater recirculation across the vast flat. A large portion (~45 %) of SGD occurring at mildly sloping beaches and potentially tidal flats is from tidal forcing (Robinson et al. 2007). The beach morphology and slope are important characteristics that affect the strength of flow and seawater recirculation in the subsurface intertidal zone and the extent of the tidal forcing; recirculation is additionally impacted by wind and terrestrial recharge (Robinson et al. 2006). The environmental setting of sloughs and mudflats in South Bay resulted in muting of

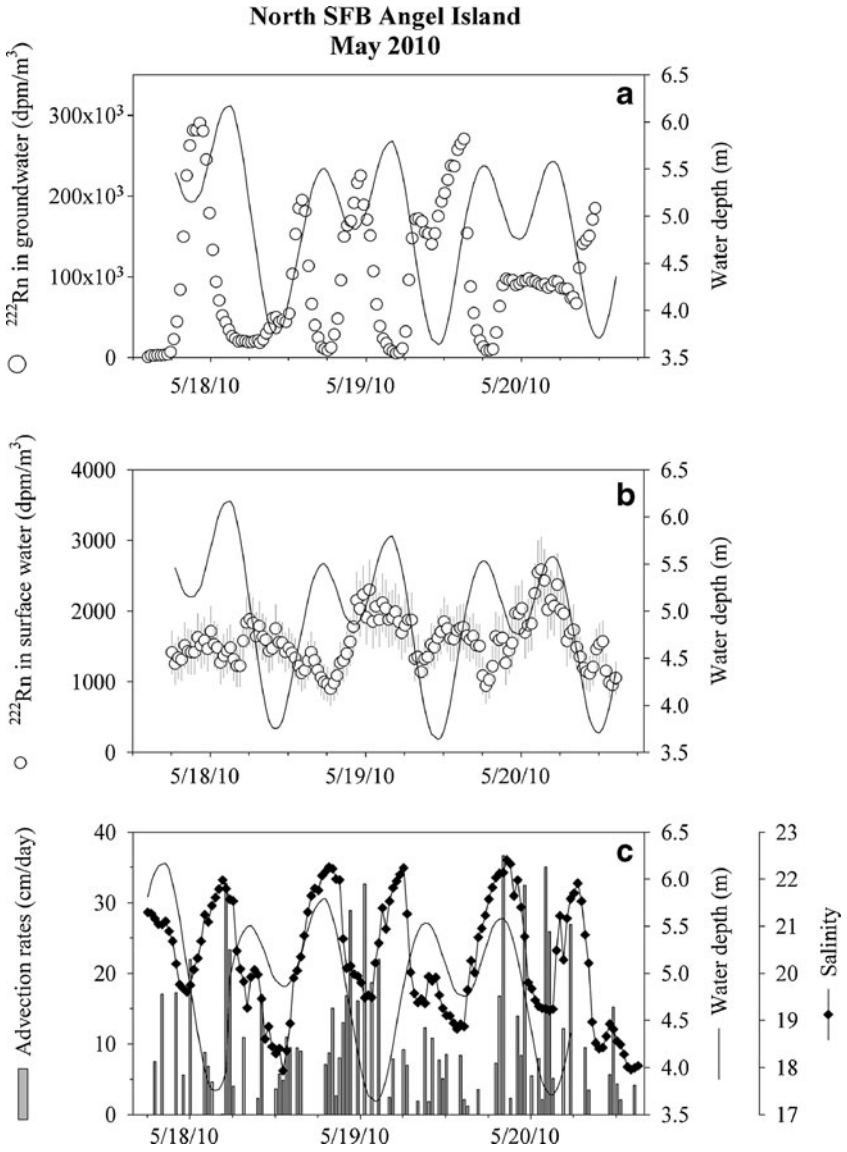

Fig. 5 **a** ^{222}Rn activity in groundwater at Angel Island versus time. **b** Complementary surface water ^{222}Rn activity versus time. **c** Calculated advection rates based on groundwater and surface water ^{222}Rn activities plotted with groundwater salinity and surface water depth over time

the tidal variability in the water record at MSI and impacted the measured Rn activities. It is possible that water in South Bay nearshore environments, particularly at MSI, is not exchanged as rapidly as at other locations and stagnant water is accumulating Rn from sediments, producing the high SGD flux. An additional factor that may impact the magnitude of the calculated SGD flux is the coastal water residence time. Our calculations produced residence times on the order of one day; however, based on the tidal regime and previous studies using a horizontal eddy diffusivity model, the residence time may be on the order of 0.5 day (Okubo 1971). Using the residence time of ~1 day calculated in this study results in more conservative SGD fluxes compared to using a residence time of 0.5 day.

A potentially important transport mechanism for Ra, Rn, and nutrients other than advective processes of SGD is diffusion from sediments. For this study, porewater gradients of Rn or Ra were not measured, and therefore, the diffusion from sediments was not calculated separately. In high energy intertidal and nearshore subtidal zones, it has been shown that fluxes of Rn and Ra are dominated by advection instead of diffusion (Rama and Moore 1996). Cable and Martin (2008) found the diffusion of Rn to account for less than 3 % of the total flux from sediments in a nearshore environment. Hammond et al. (1985) estimated bioirrigation accounted for 60 % of the flux and the remaining flux occurred via diffusion, but other advective processes particularly in the intertidal zone were not considered. Sediment characteristics and porewater concentrations are important factors affecting the importance of diffusion. At SFB, diffusion may be more important in the deep, low-energy mid-channel of SFB than in the shallow intertidal zone representing the vast area of the bay. Our estimates of SGD may therefore overestimate the magnitude

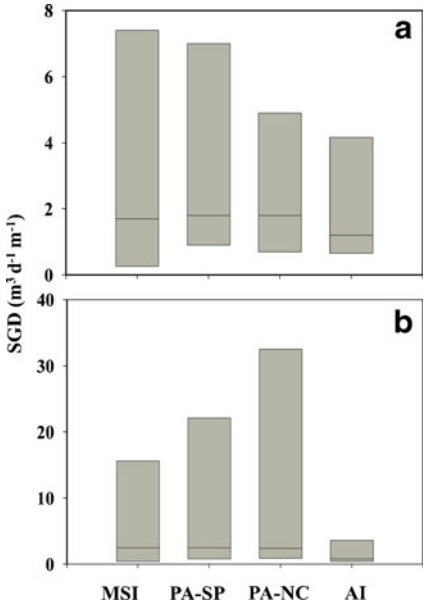

Fig. 6 SGD fluxes per meter of shoreline based on ^{224}Ra (**a**) and ^{223}Ra (**b**) activities. The *box plot* represents the range for each site and the *line* is the mean. The ranges represent the SGD flux calculated using the highest and lowest groundwater end-member ^{224}Ra or ^{223}Ra activities

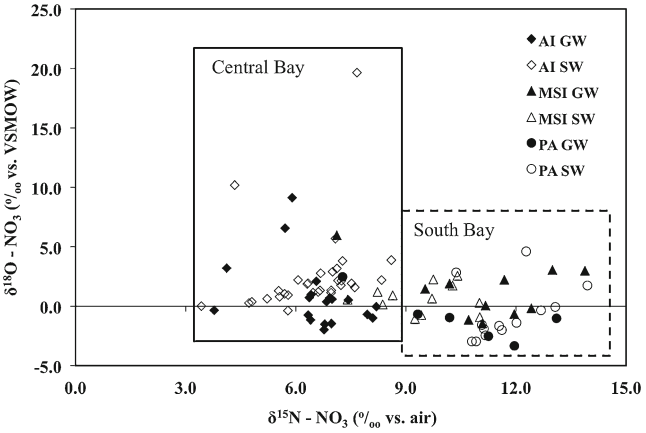

Fig. 7 Dual isotopic composition of nitrate (δ^{18}O vs. δ^{15}N) in groundwater (*GW*) and surface water (*SW*) samples at the three study sites: Marine Science Institute (*MSI*), Palo Alto Baylands (*PA*), and Angel Island (*AI*) in San Francisco Bay. *Boxes* represent the range of majority of samples for each bay (Central and South)

of *advective* flux by including the diffusional flux and should be a representative measurement of total flux. Future studies may consider comparing diffusion and advection processes of nearshore and the mid-channel environments to further our understanding of fluxes from the sediments.

SGD Derived from the Bay Basin Model

To acquire a first-order approximation of the basin scale SGD fluxes and the associated nutrient fluxes in SFB relative to other sources, we calculated SGD fluxes to the whole bay using two approaches. In the first approach, we extrapolated the fluxes calculated for a meter of shoreline based on the nearshore box fluxes described above (1.2 m^3 day^{-1} m^{-1} for Central Bay and 1.6 m^3 day^{-1} m^{-1} for South Bay) to the entire perimeter of shoreline length for each basin. The shoreline length for each basin was estimated in ArcGIS and was found to be 399,380 m for South Bay and 199,240 m for Central Bay. The resulting fluxes calculated using this first approach were 639,008 m^3 day^{-1} for South Bay and 239,088 m^3 day^{-1} for Central Bay.

In the second approach, SGD was calculated using the Ra mass balance where the activity and volume of the Central and South bay basins were used (i.e., basin mass balance). The SGD was calculated using the combined volume of Central and South Bays, 5.24×10^9 m^3 (Smith and Hollibaugh 2006), and a 60-day residence time. In the Ra mass balance calculation (Eq. 1), we used the average surface water ^{224}Ra activity for open bay waters (>20 m from shore) for both basins (A_{box}=10.9 dpm 100 L^{-1}) and the highest measured groundwater ^{224}Ra activity (A_{GW}=422 dpm 100 L^{-1}) (note that using the highest value will yield a lower estimate). We assumed that the offshore end-member had Ra activity equal to that of Pacific surface water 1 km offshore (^{223}Ra= 0.15 dpm 100 L^{-1} and ^{224}Ra=1.18 dpm 100 L^{-1}). The total flux of SGD calculated this way for the basin was 2.01×10^6 m^3 day^{-1}. This basin scale estimate is greater than the fluxes calculated by extrapolating the nearshore box model fluxes (combined flux of 0.88×10^6 m^3 day^{-1}). SGD extrapolated to the entire shoreline may produce a lower volume of

Table 3 Nutrient concentration ($NO_3^-+NO_2^-$, NH_4^+, PO_4^{3-}, $Si(OH)_4$) means and $\pm1\sigma$ for groundwater and surface waters at each site

Site		*n*	$NO_3^-+NO_2^-$ (μM)	NH_4^+ (μM)	PO_4^{3-} (μM)	$Si(OH)_4$ (μM)
MSI	Groundwater	5	48±57	61±44	12±6	161±70
	Surface	12	80±23	19±32	2.8±0.8	66±15
PA	Groundwater	12	27±29	433±288	98±107	277±76
	Surface	13	86±76	133±188	31±50	202±87
AI	Groundwater	17	123±38	2.4±1.9	4.8±1.9	128±32
	Surface	29	67±28	4.6±1.6	2.9±0.7	89±9.3

SGD due to the underestimation of the basin perimeter in ArcGIS. The many sloughs and large areas of shallow shoals increase the effective discharge zone that may not be accounted for in the ArcGIS perimeter (Jaffe and Foxgrover 2006). Another factor that may contribute to the discrepancy between the two approaches is errors associated with using an average residence time. This residence time is based on salinity balance and could vary significantly on seasonal and interannual timescales (Walters et al. 1985).

Nutrient Fluxes

Significant differences in nutrient fluxes and nitrate isotopic compositions were found between South and Central Bays. The differences in environmental settings of each basin may play a role in these differences and impact the overall nutrient loading. The positive correlations between ^{224}Ra and nutrients suggest that SGD is an important source of these nutrients to nearshore surface waters at all the sites. We calculated SGD-associated nutrient fluxes by subtracting the average surface water nutrient concentrations from the average groundwater nutrient concentrations and multiplying by the ^{224}Ra-based SGD fluxes at each site (Fig. 8). Subtracting the surface water nutrient concentration from the groundwater nutrient concentration is a conservative approach and calculates the excess nutrients associated with SGD since a significant portion of SGD is recirculated seawater. We used the SGD estimates calculated with ^{224}Ra activities to calculate nutrient fluxes as opposed to ^{223}Ra and ^{222}Rn activities because of the higher error associated with ^{223}Ra measurements and the anonymously high measurements of ^{222}Rn-based fluxes at MSI. As previously mentioned, SGD fluxes are averaged over tidal cycles, and therefore, this average carries over to the nutrient fluxes. As shown in Table 3, the concentration of the different DIN species ($NO_3^-+NO_2^-$ or NH_4^+) is site specific. Specifically, NH_4^+ was high and $NO_3^-+NO_2^-$ was low in groundwater at MSI and PA, which have broad tidally inundated muddy coastlines. At AI, where the coastline is narrow and the sediments are sandy, NH_4^+ was low, and $NO_3^-+NO_2^-$ was high (Table 3). This distribution likely results from the highly anoxic conditions in groundwater circulating through the vast tidal mudflats in the South Bay area and the more oxic groundwater at AI (Caffrey 1995). Under reducing conditions, NH_4^+ generated from organic matter decaying in the sediment will not be oxidized as it might in the oxic AI sediments. Moreover, denitrification under anoxic conditions may further lower nitrate concentrations in groundwater at MSI and PA. $NO_3^-+NO_2^-$, NH_4^+, PO_4^{3-}, and Si $(OH)_4$ fluxes were calculated for each of the sites (Fig. 8); however, as indicated above, NH_4^+ did not contribute much to the total DIN flux at AI, while $NO_3^-+NO_2^-$ did not contribute much to the total DIN at PA and MSI. It appears that groundwater is not contributing to the increase of NH_4^+ in Central Bay (Dugdale et al. 2007) but it is an important source of NH_4^+ in South Bay. In both basins, groundwater is contributing significant nutrients to surface waters that may play a role in primary productivity of the bay (see "Ecological Implications of Nutrient Loading").

If we assume that our sampling sites are representative of similar settings throughout the South and Central Bays, we can extrapolate the nutrient fluxes to the entire bay to acquire a first-order approximation of nutrient contributions associated with SGD. Applying our calculated SGD flux using the nearshore extrapolation for each basin and the excess nutrient concentration in groundwater, SGD contributed up to 113×10^3 mol NH_4^+ day^{-1} in South Bay and 13.4×10^3 mol $NO_3^-+NO_2^-$ day^{-1} in Central Bay. The PO_4^{3-} fluxes were 21.7×10^3 and 0.5×10^3 mol day^{-1} for South and Central and Bays, respectively. When the nutrient fluxes were compared to wastewater and river nutrient loading calculated by Smith and Hollibaugh (2006), we find that sewage effluent is the

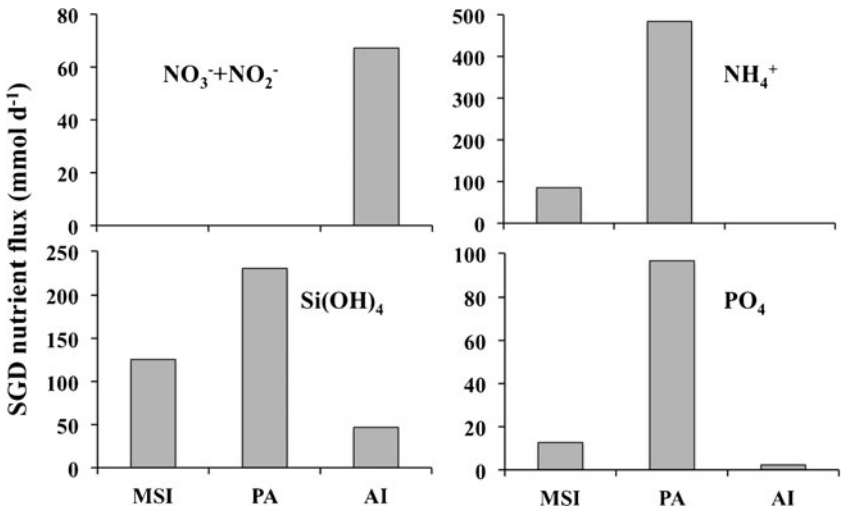

Fig. 8 Excess nutrient fluxes ($NO_3^-+NO_2^-$, NH_4^+, PO_4^{3-}, Si $(OH)_4$) per meter of shoreline for each site (MSI, PA (including PA–SP and PA–NC), and AI). Excess fluxes are calculated from ^{224}Ra-based SGD estimates. The average nutrient concentration used at each site is the surface water concentration subtracted from the groundwater concentration. Sites without *bars* indicate groundwater nutrient concentration was lower than surface water

dominant source to both bays, but SGD contributed a significant amount of nutrients as well: up to 9 % of DIN and up to 15 % of DIP in the Central and South Bays, respectively (Table 4). It should be noted that the sewage effluent and river inputs for Central Bay are estimated from San Pablo Bay values from Smith and Hollibaugh (2006) because of limited Central Bay data. Since the approach using the nearshore extrapolation may underestimate SGD and the associated flux of nutrients, we also calculated nutrient fluxes using the basin scale approach. If the SGD flux calculated using the bay basin scale (i.e., basin Ra mass balance) is applied to the average groundwater nutrient concentrations from both basins, then SGD inputs are greater and account for 16 % of DIN and 22 % of DIP when considering combined inputs to Central and South Bays (Table 4).

These nutrient flux estimates to each basin are reasonable when considering (1) previous benthic flux studies conducted in SFB (Hammond et al. 1985) and other locations and (2) that the relative contributions take into account only inputs from rivers, wastewater discharge, and SGD and do not consider other sources such as atmospheric deposition and other nonpoint sources. Sediments have been shown to be an important source of nutrients to overlying water and phytoplankton requirements, contributing up to 50 % of the nitrogen required by phytoplankton in South Bay (Grenz et al. 2000). Other shallow coastal systems have also demonstrated the importance of sediments and benthic fluxes to phytoplankton nutrient requirements (e.g., 40 % of phytoplankton nitrogen requirements in Chesapeake Bay; Boyton and Kemp 1985). Using an average benthic NH_4^+ flux in South Bay measured by Hammond et al. (1985) of 2.7 mmol m^{-2} day^{-1} and applying it to the benthic area of the basin, the resulting NH_4^+ input is 702×10^3 mol day^{-1} compared to the SGD associated NH_4^+ input of 113×10^3 mol day^{-1} in this study (Table 4). Note, however, these fluxes are calculated over different areas and using data obtained at different times. The fluxes from Hammond et al. (1985) are nutrient fluxes associated with irrigation and diffusion and assumed to be similar across the entire basin while our calculations are restricted to discharge at the coastline within the intertidal zone.

Table 4 Nutrient loading ($\times 10^3$ mol day^{-1}) and relative percent of DIN and DIP in South and Central Bays considering river, sewage, and SGD inputs

		DIN	DIP	%DIN	%DIP
Approach 1: nearshore extrapolation					
South	River	45	3	3	2
	Sewage	1,170	117	88	83
	SGD	113	22	8	15
	Total	1,328	142		
Central	River	0	0	0	0
	Sewage	130	13	91	97
	SGD	13	0.5	9	3
	Total	143	13		
Approach 2: bay basin scale					
Both	River	45	3	3	2
	Sewage	1,300	130	81	76
	SGD	261	37	16	22
	Total	1,606	170		

River and sewage inputs are estimated from Smith and Hollibaugh (2006) and SGD inputs from this study. The two approaches (1—nearshore extrapolation and 2—bay basin scale) for calculating SGD DIN and DIP fluxes are presented

DIN dissolved inorganic nitrogen, *DIP* dissolved inorganic phosphorus

As with the forcing mechanisms of SGD, it is possible that the difference in topography may impact the nutrient fluxes (i.e., nitrogen form and ratios) being discharged with SGD (Bokuniewicz et al. 2003). Steeper coastlines can support higher hydraulic gradient to drive higher SGD fluxes, and the groundwater residence time may thus be shorter. If indeed this is the case, at sites like AI, the DIN is expected to be mostly NO_3^- since there is less time for organic matter remineralization or for reducing conditions to develop in the shallow unconfined surficial aquifer. Although we did not find greater SGD at the Central Bay site with more relief, the DIN was indeed primarily in the form of NO_3^-+NO_2^-. In areas similar to South Bay, with low relief and where SGD recirculation is expected to be slow, high rates of remineralized nitrogen can be discharged (Spiteri et al. 2008). Indeed this is the situation at the South Bay sites. The concentrations of nutrient, Ra, and Rn and the associated nitrate isotope composition in groundwater may also be influenced by the short residence time of recirculated seawater in the sediments. A short residence time would provide insufficient time for porewaters to equilibrate (Burnett and Dulaiova 2003). The tidal stage (ebbing or flooding) may also impact the residence time, as it is well-known that seawater infiltration occurs during high tide and drainage during low tide (Nielsen 1990). Infiltration typically occurs faster than draining, resulting in variable porewater residence time during tidal stages for water to react with sediments and build higher concentrations (Nakada et al. 2011). Another explanation of lower-end nutrient concentrations in the groundwater samples may be the influence of pumping of groundwater during our study. Pumping can result in changes to the hydraulic head of the system and introduce low concentration surface water into our borehole, diluting the high nutrient groundwater signal. However, we used minimum pumping rates required for the method and did not sample any well that became inundated during high tide to minimize the impact of pumping.

The nitrate isotopic signature of groundwater may also proved insight to subsurface processes and transport mechanisms occurring in SFB. The similarity in NO_3^-+NO_2^- isotopic signature between groundwater and surface water

of SFB demonstrated in this study could indicate similar sources to and/or processes affecting groundwater and surface waters (Fig. 7). Specifically, in the South Bay NO_3^-+NO_2^- was enriched in ^{15}N, which is a signature of NO_3^-+NO_2^- derived from NH_4^+ following isotopic enrichment due to fractionation associated with NH_4^+ volatilization. This isotopic signature is consistent with discharge of sewage and treated wastewater, which is a likely contributor of NO_3^-+NO_2^- in the South Bay. The consistent NO_3^-+NO_2^- isotopic signature in surface water and groundwater samples suggests rapid recirculating seawater in the shallow sediments, which is the primary component of SGD in the limited freshwater system of South Bay. It is interesting to note that the DIN in the South Bay groundwater is dominated by NH_4^+ rather than NO_3^-+NO_2^-. The groundwater NH_4^+ may be oxidized after discharge and become a significant contributor to NO_3^-+NO_2^- in the South Bay surface waters. Higher uptake rates of NO_3^- in the water column in South Bay may also result in elevated isotopic values of residual NO_3^- consistent with additional fall phytoplankton blooms and increasing chlorophyll in South Bay (Cloern and Dugdale 2010). The South Bay $\delta^{15}N$-NO_3 signature was more enriched compared to the AI values as expected based on the importance of treated wastewater discharge on NO_3^-+NO_2^- concentrations in South Bay (Fig. 7). NO_3^-+NO_2^- in groundwater and surface water samples at the Central Bay site also shared a common nitrogen and oxygen isotopic composition. However, the isotope compositions at the Central Bay site are common to several potential sources of NO_3^- (marine NO_3^-, soil NO_3^-, precipitation, and some wastewaters). Thus, it is not possible to use the isotopic signature of NO_3^-+NO_2^- as a tracer of rapid seawater recirculation at the Central Bay site.

Ecological Implications of Nutrient Loading

Nutrient fluxes associated with SGD may play an important role in primary productivity in SFB. In addition to the quantity of nutrients contributed to surface waters found in this study, the nutrient form and stoichiometry may influence the phytoplankton assemblages and overall water quality. Throughout most of the year, primary productivity in the SFB is low due to light limiting conditions (Cloern and Dufford 2005) and grazing (Alpine and Cloern 1992). As a result of light limitation, dissolved nutrients are in excess and SFB is classified as a high nutrient, low chlorophyll (HNLC) environment (Cloern 2001; Jassby et al. 2002; Dugdale et al. 2007). In the Central Bay, blooms of mostly marine and brackish water diatoms and microflagellates occur in early summer (Cloern 1979; Cloern and Dufford 2005). In contrast, the South Bay has longer residence time, lower turbidity, with maximum biomass of microflagellates and small diatoms occurring in spring (Cloern 1979; Cloern et al. 1985). SGD may be playing a role in contributing excess nutrients to the system and impacting the phytoplankton assemblages.

More recent studies suggested that nutrient ratios along with irradiance might be an important factor influencing bloom events and regional ecosystem dynamics in Central Bay. Wilkerson et al. (2006) and Dugdale et al. (2007) suggested that the relative concentrations of NH_4^+ and NO_3^- can influence the phytoplankton bloom dynamics (size of phytoplankton cells and species distribution) and that excess NH_4^+ can inhibit the uptake of NO_3^- by phytoplankton. Although NH_4^+ is often a preferred source of nitrogen by phytoplankton, it seems that in Central Bay the phytoplankton community uptakes NO_3^- at higher rates and as the preferred nitrogen source to form spring blooms (Dugdale et al. 2007). Therefore, increased irradiation and decreased NH_4^+ concentrations are critical for rapid uptake of NO_3^- and bloom development in Central Bay (Dugdale et al. 2007). Elevated NH_4^+ concentrations and inhibited NO_3^- uptake have been documented in other locations, e.g., in the Delaware Bay (Pennock 1987) and in Bodega Bay, California (Dugdale et al. 2006). In contrast, it is possible that the high NH_4^+ input from SGD in South Bay is instrumental in limiting the frequency of algal blooms and contributing to maintaining the South Bay as a HNLC environment. The SGD at our Central Bay site (AI) does not contribute significant NH_4^+ to surface waters but otherwise contributes to the NO_3^- pool that could be readily taken up by phytoplankton if NH_4^+ concentrations are kept low (i.e., SGD does not contribute to inhibiting NO_3^- uptake in Central Bay).

The relative stoichiometry of discharging nutrients from sediments, such as the ratio of nitrogen and phosphorus (N:P), is also important to phytoplankton production and nutrient limitation in estuarine environments. The N:P ratio required by marine pelagic phytoplankton is typically around 16:1 ("Redfield ratio," Redfield 1934), but SGD often has higher N:P ratio (Slomp and Van Cappellen 2004) and may be important in determining the overall nutrient limitation in shallow nearshore surface water environments. The N:P ratio in SGD can be dependent on the groundwater flow rates, the form and supply of nitrogen and phosphorus, and the redox conditions of the environment immobilizing phosphorus relative to nitrogen (Slomp and Van Cappellen 2004). The N:P of groundwater in Central Bay is 28:1, similar to the surface water ratio, 25:1, when considering both NO_3^- and NH_4^+ as nitrogen sources (most of the nitrogen as NO_3^-). If we only use NH_4^+ in calculating the N:P ratio assuming NO_3^- uptake is inhibited and only NH_4^+ is bioavailable, then we find similar N:P as those recorded by Dugdale et al. (2007) in surface waters, ~ 2:1. At the South Bay sites, groundwater N:P values (using the combined NO_3^- and NH_4^+) were below the Redfield ratio, 12 and 3.5 for MSI and PA, respectively. When considering only NH_4^+ as the nitrogen form, the groundwater N:P is higher than the Central Bay but still lower than the

Redfield ratio, 4.9 and 2.3 at MSI and PA, respectively. The values in South Bay groundwater are similar to N:P ratios for SGD at other locations where reducing conditions prevail. Thus, SGD in South Bay seems to be an important source of phosphorus contributing to maintaining SFB as a nitrogen-limited system overall. The flux of the nitrogen relative to phosphate is expected to also impact phytoplankton assemblages (Hodgkiss and Ho 1997; Vrede et al. 2009) and certainly the high $Si(OH)_4$ fluxes from SGD contribute to high $Si(OH)_4$ levels in the bay and the prevalence of diatoms in this ecosystem. These data highlight the significance of SGD in SFB and the need to further investigate SGD as a nutrient source and its role in primary productivity. Specifically, SGD should be considered in future studies and management regarding eutrophication and natural or managed ecosystem changes.

Summary

Submarine groundwater discharge was quantified at select sites in SFB (South and Central Bays) using ^{223}Ra, ^{224}Ra, and ^{222}Rn measured in groundwater and surface water. SGD fluxes were similar in magnitude at the three locations in South Bay and one location in Central Bay. Although SGD fluxes were of the same order of magnitude, nutrient fluxes and particularly nitrogen forms were different between the two regions. South Bay SGD was characterized by NH_4^+ concentrations three-fold higher than open bay waters, and NH_4^+ is primary DIN form associated with SGD in South Bay. On the contrary, the primary form of DIN associated with SGD in Central Bay is NO_3^-+NO_2^-. The different DIN forms discharging from SGD may play an important role in impacting nutrient uptake rates and phytoplankton communities.

Depending on the approach used to calculate nutrient fluxes associated with SGD, SGD can account for up to 16 % of DIN and 22 % of DIP in South and Central Bays when considering river, sewage, and SGD inputs as the nutrient sources to SFB. Previous studies have identified the importance of sediment fluxes to phytoplankton nutrient requirements, but have not considered advective fluxes associated with SGD at the coastline and from tidal flats. The findings from this study indicate that nutrient loads from recirculated seawater and fresh groundwater discharge in SFB may be important for nutrient management practices in this heavily populated watershed. Although nutrients are currently not the limiting factor in phytoplankton growth in SFB, increases in phytoplankton biomass demonstrate that SFB is not resistant to nutrient pollution and changes in bay conditions can inherently increase the use of the large nutrient pool. SFB has been drastically modified and continues to undergo changes through restoration projects, freshwater input, and increased population within the watershed. Future bay changes may shift SFB to a nutrient-limited system as opposed to light limitation, and understanding sources and relative contributions of nutrients will be vital for ecosystem sustainability. Furthermore, SGD is identified as an important nutrient source and should be consider in nutrient budgets and hydrologic models to advance our understanding regarding eutrophication and ecosystem changes in estuarine and coastal systems.

Acknowledgments We would like to thank the University of California Lab Fees Research Program for funding. We would also like to thank Ellen Gray and Zhongwu Ma for assistance with fieldwork, Rob Franks at the UCSC analytical facility for help with analytical procedures, and many thanks to others that helped collect samples in the field. We extend special thanks to the park rangers and staff at Angel Island State Park for their hospitality and logistical support. PWS is grateful to the USGS Coastal and Marine Geology Program for continued support.

References

Alpine, A.E., and J.E. Cloern. 1992. Trophic interactions and direct physical effects control phytoplankton biomass and production in an estuary. *Limnology and Oceanography* 37: 946–955.

Baylosis, J.I., J.L Edmunds, B.E. Cole, and J.E. Cloern. 1997. Studies of the San Francisco Bay, California estuarine ecosystem: pilot regional monitoring results, 1996. U.S. Geological Survey Open-File Report: 97-598, 203 p.

Bokuniewicz, H., R. Buddemeier, B. Maxwell, and C. Smith. 2003. The typological approach to submarine groundwater discharge (SGD). *Biogeochemistry* 66: 145–158.

Boyton, W.R., and W.M. Kemp. 1985. Nutrient regeneration and oxygen consumption by sediments along an estuarine salinity gradient. *Marine Ecology Progress Series* 23: 45–55.

Breier, J.A., N. Nidzieko, S. Monismith, W. Moore, and A. Paytan. 2009. Tidally regulated chemical fluxes across the sediment-water interface in Elkhorn Slough, California: evidence from a coupled geochemical and hydrodynamic approach. *Limnology and Oceanography* 54: 1964–1980.

Burnett, W.C., and H. Dulaiova. 2003. Estimating the dynamics of groundwater input into the coastal zone via continuous radon-222 measurements. *Journal of Environmental Radioactivity*. doi:10.1016/S0265-931X(03)00084-5.

Burnett, W.C., H. Bokuniewicz, M. Huettel, W.S. Moore, and M. Taniguchi. 2003. Groundwater and pore water inputs to the coastal zone. *Biogeochemistry* 66: 3–33.

Burnett, W.C., P.K. Aggarwal, A. Aureli, H. Bokuniewicz, J.E. Cable, M.A. Charette, E. Kontar, S. Krupa, K.M. Kulkarni, A. Loveless, W.S. Moore, J.A. Oberdorfer, J. Oliveira, N. Ozyurt, P. Povinec, A.M.G. Privitera, R. Rajar, R.T. Ramessur, J. Scholten, T. Stieglitz, M. Taniguchi, and J.V. Turner. 2006. Quantifying submarine groundwater discharge in the coastal zone via multiple methods. *Science of the Total Environment* 367: 498–543.

Cable, J.E., and J.B. Martin. 2008. In situ evaluation of nearshore marine and fresh porewater transport into Flamengo Bay, Brazil. *Estuarine, Coastal, and Shelf Science* 76: 473–483.

Caffrey, J. 1995. Spatial and seasonal patterns in sediment nitrogen remineralization and ammonium concentrations in San Francisco Bay, California. *Estuaries and Coasts* 18: 219–233.

Charette, M.A., K.O. Buesseler, and J.E. Andrews. 2001. Utility of radium isotopes for evaluating the input and transport of

groundwater-derived nitrogen to a Cape Cod Estuary. *Limnology and Oceanography* 46: 465–470.

Chin, J.L., D.L. Woodrow, M. McGann, F.L. Wong, T. Fregoso, and B.E. Jaffe. 2010. Estuarine sedimentation, sediment character, and foraminiferal distribution in central San Francisco Bay, California: U.S. Geological Survey Open-File Report 2010-1130: 58 p.

Cloern, J.E. 1979. Phytoplankton ecology of the San Francisco bay system: The status of our current understanding. In *San Francisco Bay: the urbanized estuary*, ed. T.J. Conomos, 247–264. San Francisco: Pacific Division, AAAS.

Cloern, J.E. 2001. Our evolving conceptual model of the coastal eutrophication problem. *Marine Ecology Progress Series* 211: 223–253.

Cloern, J.E., and R. Dufford. 2005. Phytoplankton community ecology: principles applied in San Francisco Bay. *Marine Ecology Progress Series* 285: 11–28.

Cloern, J.E. and R. Dugdale. 2010. San Francisco Bay. In *Nutrients in estuaries: A summary report of the National Estuarine Experts Workgroup 2005–2007*, ed. P.M. Glibert et al., 117–126. Washington, DC: USEPA.

Cloern, J.E., B.E. Cole, R.L.J. Wong, and A.E. Alpine. 1985. Temporal dynamics of estuarine phytoplankton: A case study of San Francisco Bay. *Hydrobiologia* 129: 153–176.

Cloern, J.E., B.E. Cole, J.L. Edmunds, T.S. Schraga, and A. Arnsberg. 2000. Patterns of water-quality variability in San Francisco Bay during the first six years of the regional monitoring program, 1993–1998, in 1998 Annual Report, San Francisco estuary regional monitoring program for trace substances: San Francisco Estuary Institute: 20 p.

Cloern, J.E., A.D. Jassby, J.K. Thompson, and K.A. Hieb. 2007. A cold phase of the East Pacific triggers new phytoplankton blooms in San Francisco Bay. *Proceedings of the National Academies of Science*. doi:10.1073/pnas.0706151104.

Conomos, T.J., and D.H. Peterson. 1977. *Suspended-particle transport and circulation in San Francisco Bay: An overview. Estuarine processes vol. 2; circulation, sediments, and transfer of material in the estuary*, 82–97. New York: Academic.

Conomos, T.J., R.E. Smith, and J.W. Gartner. 1985. Environmental setting of San Francisco Bay. *Hydrobiologia* 129: 1–12.

Corbett, D.R., J. Chanton, W. Burnett, K. Dillon, C. Rutkowski, and J.W. Fourqurean. 1999. Patterns of groundwater discharge into Florida Bay. *Limnology and Oceanography* 44: 1045–1055.

de Sieyes, N.R., K.M. Yamahara, B.A. Layton, E.H. Joyce, and A.B. Boehm. 2008. Submarine discharge of nutrient-enriched fresh groundwater at Stinson Beach, California is enhanced during neap tides. *Limnology and Oceanography* 53: 1434–1445.

Dugdale, R.C., F.P. Wilkerson, A. Marchi, and V. Hogue. 2006. Nutrient controls on new production in the Bodega Bay, California, coastal upwelling plume. *Deep-Sea Research II* 53: 3049–3062.

Dugdale, R.C., F.P. Wilkerson, V.E. Hogue, and A. Marchi. 2007. The role of ammonium and nitrate in spring bloom development in San Francisco Bay. *Estuarine, Coastal, and Shelf Science* 73: 17–29.

Garcia-Solsona, E., J. Garcia-Orellana, P. Masque, and H. Dulaiova. 2008. Uncertainties associated with 223Ra and 224Ra measurements in water via a delayed coincidence counter (RaDeCC). *Marine Chemistry*. doi:org/10.1016/j.marchem.2007.11.006.

Garrison, G.H., C.R. Glenn, and G.M. McMurtry. 2003. Measurement of submarine groundwater discharge in Kahana Bay, O'ahu, Hawai'i. *Limnology and Oceanography* 48: 920–928.

Grenz, C., J.E. Cloern, S.W. Hager, and B.E. Cole. 2000. Dynamics of nutrient cycling and related benthic nutrient and oxygen fluxes during a spring phytoplankton bloom in South San Francisco Bay (USA). *Marine Ecology Progress Series* 197: 67–80.

Hammond, D.E., and C. Fuller. 1979. The use of radon-222 to estimate benthic exchange and atmospheric exchange rates. In *San Francisco Bay, the urbanized estuary*, ed. T.J. Conomos, 213–230. Washington, D. C.: Pacific Division of the American Association for the Advancement of Science.

Hammond, D.E., C. Fuller, D. Harmon, B. Hartman, M. Korosec, L.G. Miller, R. Rea, S. Warren, W. Berelson, and S.W. Hager. 1985. Benthic fluxes in San Francisco Bay. *Hydrobiologia* 129: 69–90.

Hartman, B., and D.E. Hammond. 1984. Gas exchange rates across the sediment–water and air–water interfaces in south San Francisco Bay. *Journal of Geophysical Research* 89: 3593–3603.

Hodgkiss, I.J., and K.C. Ho. 1997. Are changes in N:P ratios in coastal waters the key to increased red tide blooms? *Hydrobiologia*. doi:10.1023/A:1003046516964.

Hsu, K., and M. Stacey. 2011. *Exchange between an estuary and an intertidal marsh and slough*. Daytona Beach: Coastal and Estuarine Research Federation.

Hwang, D., G. Kim, Y. Lee, and H. Yang. 2005. Estimating submarine inputs of groundwater and nutrients to a coastal bay using radium isotopes. *Marine Chemistry* 96: 61–71.

Jaffe, B. and A. Foxgrover. 2006. A history of intertidal flat area in South San Francisco Bay, California: 1858 to 2005. USGS Open-File Report 2006-1262.

Jassby, A.D., J.E. Cloern, and B.E. Cole. 2002. Annual primary production: patterns and mechanisms of change in a nutrient-rich tidal ecosystem. *Limnology and Oceanography* 47: 698–712.

Kennish, M.J. 2001. Coastal salt marsh systems in the U.S.: A review of anthropogenic impacts. *Journal of Coastal Research* 17: 731–748.

Knee, K.L., B.A. Layton, J.H. Street, A.B. Boehm, and A. Paytan. 2008. Sources of nutrients and fecal indicator bacteria to nearshore waters on the North Shore of Kaua'i (Hawai'i, USA). *Estuaries and Coasts*. doi:10.1007/s12237-008-9055-6.

Knee, K.L., J.H. Street, E.E. Grossman, A.B. Boehm, and A. Paytan. 2010. Nutrient inputs to the coastal ocean from submarine groundwater discharge in a groundwater-dominated system: relation to land use (Kona coast, Hawaii, U.S.A.). *Limnology and Oceanography*. doi:10.4319/lo.2010.55.3.1105.

Knowles, N., and D.R. Cayan. 2002. Potential effects of global warming on Sacramento/San Joaquin watershed and the San Francisco estuary. *Geophysical Research Letters*. doi:10.1029/2001GL014339.

Krest, J.M., and J.W. Harvey. 2003. Using natural distributions of short-lived radium isotopes to quantify groundwater discharge and recharge. *Limnology and Oceanography* 48: 290–298.

Krest, J.M., W.S. Moore, L.R. Gardner, and J.T. Morris. 2000. Marsh nutrient export supplied by groundwater discharge: evidence from radium measurements. *Global Biogeochemical Cycles* 14: 167–176.

Mao, X., P. Enot, D.A. Barry, L. Li, A. Binley, and D.S. Jeng. 2006. Tidal influence on behavior of a coastal aquifer adjacent to a low-relief estuary. *Journal of Hydrology*. doi:10.1016/j.jhydrol.2005.11.030.

Michael, H.A., A.E. Mulligan, and C.F. Harvey. 2005. Seasonal oscillations in water exchange between aquifers and the coastal ocean. *Nature*. doi:10.1038/nature03935.

Moore, W.S. 1976. Sampling ^{228}Ra in the deep ocean. *Deep Sea Research and Oceanographic Abstracts* 23: 647–651.

Moore, W.S. 1996. Large groundwater inputs to coastal waters revealed by ^{226}Ra enrichments. *Nature* 380: 612–614.

Moore, W.S. 1999. The subterranean estuary: A reaction zone of ground water and seawater. *Marine Chemistry* 65: 111–125.

Moore, W.S. 2000. Ages of continental shelf water determined from ^{223}Ra and ^{224}Ra. *Journal of Geophysical Research* 105: 22,117–22,122.

Moore, W.S. 2003. Sources and fluxes of submarine groundwater discharge delineated by radium isotopes. *Biogeochemistry* 66: 75–93.

Moore, W.S. 2010. The effect of submarine groundwater discharge on the ocean. *Annual Review of Marine Science*. doi:10.1146/annurev-marine-120308-081019.

Moore, W.S., and R. Arnold. 1996. Measurement of 223Ra and 224Ra in coastal waters using a delayed coincidence counter. *Journal of Geophysical Research* 101: 1321–1329.

Moore, W.S., and J. de Oliveira. 2008. Determination of residence time and mixing processes of the Ubatuba, Brazil, inner shelf waters using natural Ra isotopes. *Estuarine, Coastal, and Shelf Science* 76: 512–521.

Nakada, S., J. Yasumoto, M. Taniguchi, and T. Ishitobi. 2011. Submarine groundwater discharge and seawater circulation in a subterranean estuary beneath a tidal flat. *Hydrologic Processes*. doi:10.1002/hyp.8016.

Nichols, F.H., J.E. Cloern, S.N. Luoma, and D.H. Peterson. 1986. The modification of an estuary. *Science*. doi:10.1126/science.231.4738.567.

Nielsen, P. 1990. Tidal dynamics of the water table in beaches. *Water Resources Research* 26: 2127–2134.

Null, K.A., D.R. Corbett, D.J. DeMaster, J.M. Burkholder, C.J. Thomas, and R.E. Reed. 2011. Porewater advection of ammonium into the Neuse River Estuary, North Carolina, USA. *Estuarine, Coastal, and Shelf Science*. doi:10.1016/j.ecss.2011.09.016.

Okubo, A. 1971. Oceanic diffusion diagrams. *Deep-Sea Research* 18: 789–802.

Paerl, H.W. 2009. Controlling eutrophication along the freshwater–marine continuum: dual nutrient (N and P) reductions are essential. *Estuaries and Coasts*. doi:10.1007/s12237-009-9158-8.

Paytan, A., G.G. Shellenbarger, J.H. Street, M.E. Gonneea, K. Davis, M.B. Young, and W.S. Moore. 2006. Submarine groundwater discharge: an important source of new inorganic nitrogen to coral reef ecosystems. *Limnology and Oceanography* 51: 343–348.

Pennock, J.R. 1987. Temporal and spatial variability in phytoplankton ammonium and nitrate uptake in the Delaware Bay. *Estuarine, Coastal and Shelf Science* 24: 841–857.

Porterfield, G. N., L. Hawley and C. A. Dunnam. 1961. Fluvial sediments transported by streams tributary to the San Francisco Bay area. U.S. Geol. Survey Open-File Rep., 70 pp.

Rama, and W.S. Moore. 1996. Using the radium quartet for evaluating groundwater input and water exchange in salt marshes. *Geochimica et Cosmochimica Acta* 60: 4645–4652.

Redfield, A.C. 1934. On the proportions of organic derivatives in seawater and their relation to the composition of plankton. In *James Johnson memorial volume*, ed. R.J. Daniel, 177–192. Liverpool: Liverpool Univ. Press.

Robinson, C., B. Gibbes, and L. Li. 2006. Driving mechanisms for groundwater flow and salt transport in a subterranean estuary. *Geophysical Research Letters*. doi:03410.01029/02005GL025247.

Robinson, C., L. Li, and D.A. Barry. 2007. Effect of tidal forcing on a subterranean estuary. *Advances in Water Resources* 30: 851–865.

Schoellhamer, D.H. 2011. Sudden clearing of estuarine waters upon crossing the threshold from transport to supply regulation of sediment transport as an erodible sediment pool is depleted: San Francisco Bay, 1999. *Estuaries and Coasts*. doi:10.1007/s12237-011-9382-x.

Shellenbarger, G.G., S. Monismith, A. Genin, and A. Paytan. 2006. The importance of submarine groundwater discharge to the nearshore nutrient supply in the Gulf of Aqaba (Israel). *Limnology and Oceanography* 51: 1876–1886.

Sigman, D.M., K.L. Casciotti, M. Andreani, C. Barford, M. Galanter, and J.K. Bohlke. 2001. A bacterial method for the nitrogen isotopic analysis of nitrate in seawater and freshwater. *Analytical Chemistry*. doi:10.1021/ac010088e.

Singleton, M.J., K.N. Woods, M.E. Conrad, D.J. Depaolo, and P.E. Dresel. 2005. Tracking sources of unsaturated zone and groundwater nitrate contamination using nitrogen and oxygen stable isotopes at the Hanford Site, Washington. *Environmental Science Technology*. doi:10.1021/es0481070.

Slomp, C.P., and P. Van Cappellen. 2004. Nutrient inputs to the coastal ocean through submarine groundwater discharge: controls and potential impact. *Journal of Hydrology* 295: 64–86.

Smith, S.V., and J.T. Hollibaugh. 2006. Water, salt, and nutrient exchanges in San Francisco Bay. *Limnology and Oceanography* 51: 504–517.

Spinelli, G.A., A.T. Fisher, C.G. Wheat, M.D. Tryon, K.M. Brown, and A.R. Flegal. 2002. Groundwater seepage into northern San Francisco Bay: implications for dissolved metals budgets. *Water Resources Research*. doi:10.1029/2001WR000827.

Spiteri, C., C.P. Slomp, M.A. Charette, K. Tuncay, and C. Meile. 2008. Flow and nutrient dynamics in a subterranean estuary (Waquoit Bay, MA, USA): field data and reactive transport modeling. *Geochimica et Cosmochimica Acta* 72: 3398–3412.

Swarzenski, P.W., and J.A. Izbicki. 2009. Coastal groundwater dynamics off Santa Barbara, California: combining geochemical tracers, electromagnetic seepmeters, and electrical resistivity. *Estuarine, Coastal, and Shelf Science*. doi:10.1016/j.ecss.2009.03.027.

Swarzenski, P.W., C. Reich, K. Kroeger, and M. Baskaran. 2007. Ra and Rn istotopes as natural tracers of submarine groundwater discharge in Tampa Bay, Florida. *Marine Chemistry*. doi:10.1016/j.marchem.2006.08.001.

Taniguchi, M., W.C. Burnett, J.E. Cable, and J.V. Turner. 2002. Investigation of submarine groundwater discharge. *Hydrologic Processes* 16: 2115–2129.

Taniguchi, M., T. Ishitobi, W. Burnett, and G. Wattayakorn. 2007. Evaluating ground water-sea water via resistivity and seepage meters. *Ground water*. doi:10.1111/j.1745-6584.2007.00343.x.

Taniguchi, M., T. Ishitobi, and J. Shimada. 2006. Dynamics of submarine groundwater discharge and freshwater–seawater interface. *Journal of Geophysical Research*. doi:10.1029/2005JC002924.

Valiela, I., J. Costa, K. Foreman, J. Teal, B. Howes, and D. Aubrey. 1990. Transport of groundwater-borne nutrients from watersheds and their effects on coastal waters. *Biogeochemistry*. doi:10.1007/BF00003143.

Valiela, I., K. Foreman, M. Lamontagne, D. Hersh, J. Costa, P. Peckol, B. DeMeo-Anderson, C. D'Avanzo, M. Babione, and C.C. Sham. 1992. Couplings of watersheds and coastal waters: sources and consequences of nutrient enrichment in Waquoit Bay, Massachusetts. *Estuaries and Coasts*. doi:10.2307/1352389.

Vrede, T., A. Ballantyne, C. Mille-Lindblom, G. Algesten, C. Gudasz, S. Lindahl, and A.K. Brunberg. 2009. Effects of N:P loading ratios on phytoplankton community composition, primary production and N fixation in a eutrophic lake. *Freshwater Biology* 54: 331–344.

Walters, R.A., R.T. Cheng, and J.T. Conomos. 1985. Time scales of circulation and mixing processes of San Francisco Bay waters. *Hydrobiologia* 129: 13–36.

Wankel, S.D., C. Kendall, C.A. Francis, and A. Paytan. 2006. Nitrogen sources and cycling in the San Francisco Bay estuary: A nitrate dual isotopic composition approach. *Limnology and Oceanography* 51: 1654–1664.

Wilkerson, F., R. Dugdale, V. Hogue, and A. Marchi. 2006. Phytoplankton blooms and nitrogen productivity in San Francisco Bay. *Estuaries and Coasts* 29: 401–416.